AECL—7900
Radiation Effects, 1983, Vol. 70, pp. 197-216
0033-7579/83/7004-0197$18.50/0

AXIAL DECHANNELING OF MeV PROTONS IN GOLD

L. M. HOWE, J. A. MOORE†, N. MATSUNAMI‡
and D. R. WRIGHT§

Solid State Science Branch, Atomic Energy of Canada Limited Research Company, Chalk River, Ontario, Canada K0J 1J0

(*Received July 15, 1982*)

Dechanneling of 0.5–2.0 MeV protons incident along the ⟨110⟩ axis of high quality gold crystals has been investigated for crystal temperatures ranging from 35 to 275 K. The normalized yield $\chi(z)$ (i.e. the random fraction) was obtained from the experimental aligned and random spectra using a numerical method. Account was taken of the difference in stopping power between channeled and random trajectories, the variation of stopping power and scattering cross section with energy and the deviation of backscattered spectra from single scattering theory. Theoretical dechanneling curves were obtained using the diffusion model treatment of Matsunami and Howe. In the theoretical treatment the electron density ρ_0 around the center of the channel is taken into account in the electronic scattering and a correction factor C_n is applied for the nuclear scattering. Good agreement theory and experiment was obtained for ρ_0 values in the region 0.8–1.0 electrons Å^{-3}.

1 INTRODUCTION

The dechanneling of MeV ions in single crystals has been studied fairly extensively.[1–6] The most detailed work has been on light ions (^{1}H, ^{4}He) in silicon. In recent studies,[4–6] the theoretical analysis is based on a diffusion model in which the change with depth of the distribution in transverse energy of the channeled ions is described by a diffusion equation. The effect of dechanneling of the ions by any residual defects is assumed to be negligible. Good agreement between the theoretical calculations and the experimental data (10–20%) has been reported in a number of cases, e.g. for ^{1}H and ^{2}H in Si[5,6] and Ge.[6] In the diffusion model developed by Matsunami and Howe,[6] analytical expressions have been derived for the diffusion functions associated with scattering of the ion beam by electrons and by lattice vibrations, and also for other functions, such as the accessible area and the initial distribution of channeled ions, which are required for solving the diffusion equation. The diffusion equation is then solved numerically. This diffusion model can be fairly readily applied to the description of dechanneling in different projectile-target systems as a function of crystal temperature and incident ion energy.

Gold has a lower Debye temperature (170 K) and a considerably different electronic configuration than either Si or Ge. Consequently, the rate of change in the transverse energy distribution, and hence the dechanneling due to nuclear and electron

†Present address: Physics Department, Brock University, St. Catharines, Ontario, Canada.
‡Present address: Department of Crystalline Materials Science, Nagoya University, Nagoya, Japan.
§Present address: Max Planck Institut, Berlin, Germany.

scattering will be quite different in Au from that in Si and Ge. For example, the dechanneling rate in Au should be much more strongly temperature dependent in the low temperature range, 35 to 275 K, than is the case for Si and Ge. Dechanneling in Au should therefore provide a further test of the validity of the dechanneling theory described by Matsunami and Howe.[6] This paper reports on the dechanneling of protons in ⟨110⟩ Au as a function of crystal temperature and incident beam energy and compares the experimental results with theoretical calculations obtained using the diffusion model of Matsunami and Howe.[6]

In the experimental determination of dechanneling in crystals, there are two important factors which require careful consideration: (1) the degree of perfection of the single crystal and (2) the analysis of the aligned and random spectra to determine the normalized yield $\chi(z)$ as a function of depth z. This paper describes the preparation and characterization of Au samples sectioned from single crystals grown from the melt and presents the data which strongly support the assumption made in the subsequent theoretical analysis that the dechanneling produced by any residual lattice defects is negligible. Special consideration has been given to the determination of $\chi(z)$ from the aligned and random backscattered spectra. This resulted in the development of a self-consistent numerical analysis which systematically takes into account the difference in stopping power between channeled and random trajectories, the variation of stopping power and scattering cross section with energy and a significant deviation of backscattered spectra from single scattering theory which is observed in the case of MeV protons incident on Au. The details of this numerical analysis are given in a recent publication.[7]

2 EXPERIMENTAL PROCEDURE

Gold crystals were grown by the Bridgman method and then annealed at 1175 K for 24 h in a vacuum of 7×10^{-4} Pa. Disc shaped samples, 7–10 mm in diameter and 2–3 mm thick were cut by spark erosion from the Au single crystals. In order to remove the damage sustained in the surface region during the spark cutting operation, the discs were mechanically polished on successively finer emery papers and then on cloth wheels using diamond paste of graded sizes down to 0.25 μm, vibratory polished for 24 h in a slurry consisting of water and 0.05 μm Al_2O_3 particles and finally electropolished at a rate of approximately 1 μm per minute for several minutes. The electrolyte used for electropolishing consisted of a mixture of 135 cm^3 glacial acetic acid, 22 g chromic acid and 7 cm^3 H_2O. The crystals were then subjected to further annealing treatments to ensure the attainment of a high degree of crystal perfection. This was accomplished by first cleaning the polished crystals in hot trichlorethylene, acetone and alcohol and then annealing at a temperature approximately 50 K below the melting point (1336 K) for 80–100 h in a vacuum of $\sim7\times10^{-6}$ Pa. The annealed crystals were then cooled very slowly to room temperature at a controlled rate of 10–20 K per h. Just prior to the channeling investigations the annealed crystals were re-electropolished.

The dechanneling measurements were performed in the low temperature target chamber[8] of the 2.5 MV Chalk River Van de Graaff accelerator using the backscattering of $^1H^+$ ions. The crystals were mounted on a goniometer and then cooled to 35 K in the low temperature chamber by means of a refrigeration unit. A cryoshield at 20 K surrounded the crystal to reduce condensation of residual gases onto the crystal surface. Temperatures were varied between 35 K and 275 K by means

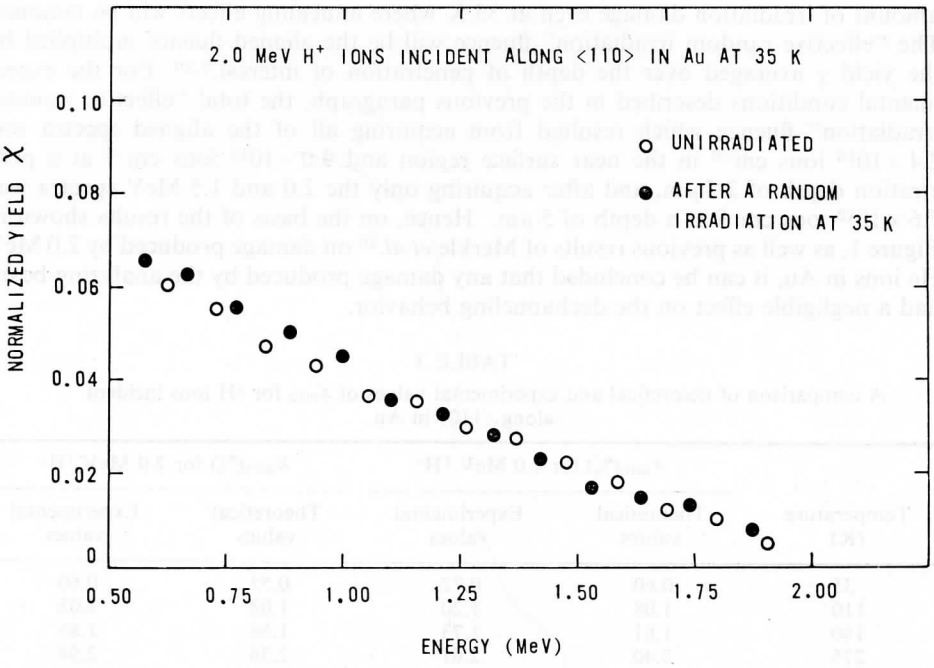

FIGURE 1 The normalized yield $\chi(z)$ as a function of the energy of protons (incident energy 2.0 MeV) backscattered from a Au crystal before and after a random irradiation (6.4×10^{13}, 2 MeV ^{1}H ions cm^{-2}) at 35 K.

of a heater attached to the crystal holder. The analyzing beam was approximately 1 mm in diameter and had a divergence of $\pm 0.03°$. Energies of backscattered ions were measured using a surface barrier detector mounted in a vertical plane with respect to the crystal and at a scattering angle of 150°. The ion fluence was measured by integrating the current collected by the sample. To suppress secondary electrons, the shield was maintained at a negative bias of 90 V with respect to the sample.

Preliminary alignment of the crystal was performed using a 2 MeV proton beam. The beam was then moved to a different position on the crystal surface, the crystal alignment was quickly checked and a series of backscattering spectra were recorded. To minimize the effect of the analyzing beam damage, the measurements of aligned spectra were made in order of decreasing energy; at each energy the temperature was varied between 35 K and 275 K. Random spectra were measured following completion of the aligned beam measurements. Typically, proton beam fluences were 1.3×10^{14} and 6.4×10^{13} ions cm^{-2} for each aligned and random spectrum, respectively.

An assessment of the damaging effect of the analyzing beam was obtained in a separate experiment. Figure 1 shows two aligned energy spectra for 2 MeV ^{1}H ions incident along $\langle 110 \rangle$ in Au at 35 K, one spectrum obtained on an unirradiated portion of the crystal and the other following irradiation of the crystal in a random crystallographic direction with 2 MeV protons to a fluence of 6.4×10^{13} ions cm^{-2} (the normal fluence received during the recording of a random spectrum). It is evident from Figure 1 that such an analyzing beam fluence produces a negligible

amount of irradiation damage even at 35 K where annealing effects will be minimal. The "effective random irradiation" fluence will be the aligned fluence multiplied by the yield χ averaged over the depth of penetration of interest.[9,10] For the experimental conditions described in the previous paragraph, the total "effective random irradiation" fluence which resulted from acquiring all of the aligned spectra was 2.4×10^{13} ions cm^{-2} in the near surface region and 9.0×10^{13} ions cm^{-2} at a penetration depth of 2.5 μm, and after acquiring only the 2.0 and 1.5 MeV spectra was 7.6×10^{13} ions cm^{-2} at a depth of 5 μm. Hence, on the basis of the results shown in Figure 1, as well as previous results of Merkle *et al.*[10] on damage produced by 2.0 MeV He ions in Au, it can be concluded that any damage produced by the analyzing beam had a negligible effect on the dechanneling behavior.

TABLE I

A comparison of theoretical and experimental values of χ_{min} for ^{1}H ions incident along ⟨110⟩ in Au

Temperature (K)	χ_{min}(%) for 1.0 MeV $^1H^+$		χ_{min}(%) for 2.0 MeV $^1H^+$	
	Theoretical values	Experimental values	Theoretical values	Experimental values
35	0.60	0.72	0.53	0.60
110	1.08	1.20	1.02	1.03
180	1.61	1.73	1.56	1.85
275	2.40	2.61	2.36	2.94

3 RESULTS AND DISCUSSION

3.1 *Assessment of the Quality of the Au Single Crystals*

Initial assessment of the quality of the single crystal was made by X-ray and reflection electron diffraction. However, in the final selection of samples suitable for the present studies we relied on the conclusions drawn from the analysis of channeling data; this is described below.

Backscattering spectra were obtained for 1 MeV ^{1}H ions incident along ⟨110⟩ for three samples cut from two different Au crystals. At 35 K, the dechanneling rates (slope of normalized yield χ versus depth z plot) for the different crystals were within 30% of one another and at 275 K the dechanneling rates were the same within the precision of measurement (5%). The crystal exhibiting the lowest dechanneling rates was selected for the detailed study. Additional checks on this crystal revealed no significant difference (i.e. $\lesssim$5%) in dechanneling behavior from different areas on the surface of the crystal. A further detailed assessment of the degree of perfection of this crystal now follows.

Shown in Table I, are the experimentally observed and theoretical values for χ_{min}, the minimum value in the aligned yield, as a function of temperature for protons incident along ⟨110⟩ in Au. The measured value for χ_{min} is given by

$$\chi_{min} = N_a/N_r \tag{1}$$

where N_a and N_r are the aligned and random yields evaluated at the same backscattered energy. This expression for χ_{min} is valid under the assumption that the

TABLE II

A comparison of theoretical and experimental values of $\psi_{1/2}$ for ^{1}H ions incident along $\langle 110 \rangle$ in Au

Energy (MeV)	Temperature (K)	$\psi_{1/2}$ (degrees)	
		Theoretical values	Experimental values
1.0	35	1.44	1.46
0.5	275	1.47	1.53
1.0	275	1.04	0.95
1.5	275	0.85	0.88
2.0	275	0.74	0.62

energy loss factors for the aligned and random spectra are the same in the near-surface region. In Table I, the measured values for $\chi_{\min}$ are averaged over approximately 50–150 nm in order to exclude any contribution from the surface peak and to properly compare with theoretical results. Table II gives the variation of $\psi_{1/2}$, the axial dip half-angle, with energy and temperature. The theoretical values for $\chi_{\min}$ and $\psi_{1/2}$ have been calculated using Barrett's formulation[11] which represents a fit to the results of Monte Carlo calculations. The theoretical value of $\chi_{\min}$ was obtained using the expression[11]

$$\chi_{\min} = C(\Delta) N d \pi u_2^2 (1 + \xi^{-2})^{1/2} \tag{2}$$

where N is the atomic density, d is the spacing between atoms in the row, u_2 is the root-mean-square thermal displacement in a plane and $C(\Delta)$ is a coefficient whose value depends on the variance Δ of the Gaussian distribution of the beam directions used in the simulations (for $\Delta=0$, $C(\Delta)=3.0\pm0.2$).[11] ξ is given by

$$\xi = 2.2\, u_1/(\psi_{1/2} d) \tag{3}$$

where u_1 is the root-mean-square thermal displacement in one direction (i.e. $u_1=u_2/\sqrt{2}$). Based on Barrett's calculations,[11] the expression which was considered appropriate for calculating the half-angle of the angular dip was

$$\psi_{1/2} = 0.80\, (2Z_1 Z_2 e^2/dE)^{1/2}\, [f(1.2\, u_1/a)]^{1/2} \tag{4}$$

where Z_1 and Z_2 are the atomic numbers of the channeled ions and crystal atoms respectively, e is the electronic charge, E is the incident energy of the ion beam, a is a screening radius (0.0102 nm for protons in Au), and $f(1.2\, u_1/a)$ is a function of the interatomic potential chosen (see Table I in Ref. 11).

Thermal vibrational amplitudes for Au were determined from the Debye model using a value of 170 K for the Debye characteristic temperature.[12] The calculated values of u_1 were 0.0037, 0.0054, 0.0069 and 0.0085 nm at 35, 110, 180 and 275 K, respectively.

From Table I it can be seen that all the experimental $\chi_{\min}$ values lie within 25% of the theoretical values and in many cases are within 10%. Similarly, as shown in Table II, the experimental $\psi_{1/2}$ values generally lie within 10% of the theoretical values.

To examine the surface region of the Au single crystal with better depth resolution, ^{4}He ion beams were used. Strong temperature dependence of surface peaks was

TABLE III

A comparison of the experimental values for A_p for ^{4}He ions incident along ⟨110⟩ in Au with values expected from a "best fit" to experimental data for other crystals

Energy (MeV)	Temperature (K)	A_p (atoms/row) Present experimental values for Au	A_p (atoms/row) "Best fit" values for 1×1 surfaces	u_2/R_M
2.0	40	1.79	1.40	0.529
1.0	40	1.30	1.25	0.394
1.0	300	2.61	2.70	0.905

observed. There was also evidence of oscillations in the aligned yield with depth, just below the surface peak, thus indicating a well-ordered surface.[11]

Values of the surface peak area A_p, expressed as atoms per row, are listed in Table III for ^{4}He ions incident along ⟨110⟩. For the Au crystal the surface normal was ~9° from the ⟨110⟩ axis. A_p was determined by a direct comparison of the backscattered intensity from the aligned Au sample and from a standard sample[13] of Si implanted with Bi. Specifically, A_p was calculated from

$$A_p = (1/1.7 \times 10^{15})\,(Y_{Au}/Y_{Bi})\,(Z_{Bi}/Z_{Au})^2(n) \tag{5}$$

where Y_{Au} and Y_{Bi} are the number of counts integrated through the surface peak for the Au crystal and Si(Bi) standard, respectively, Z_{Au} and Z_{Bi} are the atomic numbers, n is the number of Bi atoms cm^{-2} in the standard target and 1.7×10^{15} is the number of Au ⟨110⟩ rows cm^{-2}. Also given in Table III are the "best fit" values of A_p interpolated from a plot[14] of A_p versus u_2/R_M based on Rutherford backscattering measurements on various crystals having surfaces which were atomically clean and which exhibit a 1×1 LEED pattern. R_M is the calculated distance-of-closest approach where the ion flux at the second atom in the atomic row falls to zero.[14] The "best fit" values should represent a very good estimate of A_p for a Au surface which has the same structure as the bulk of the crystal. The reasonably good agreement between the experimentally observed and the "best fit" values shows that the surface structure of the Au crystal is essentially identical to the bulk structure.

From the above results it can be concluded that the Au crystal used for the detailed dechanneling study exhibited a high degree of perfection.

3.2 *Determination of the Normalized Yield* χ(z)

$\chi(z)$ is normally calculated directly, but approximately, from the ratio of the aligned to random yields.[5] Examples of dechanneling curves obtained using this method are given in Figure 2; as indicated by the open symbol data points. The depth scale was calculated from the energy loss ΔE of the beam in penetrating to a distance z along the beam path[15]

$$\Delta E = K_{M_2}\int_0^z S(E_1)\mathrm{d}z + \int_0^{z/\cos\theta} S(E_2)\mathrm{d}z \tag{6}$$

a value close to half the random stopping power was used. Similarly in the present investigation, it was assumed that $S(E_1)=0.5\,S(E_2)$. Values for the random stopping power were taken from the tabulations of Andersen and Ziegler.[17] In obtaining the energy to depth conversion, a computer program was employed in which the backscattered energy was determined successively in small depth increments, with the stopping power appropriate to each successive depth increment being used in the calculation.

Recently,[7] a numerical method has been formulated which should lead to a better evaluation of $\chi(z)$. It provides a self-consistent analysis which systematically takes into account the difference in stopping power between channeled and random trajectories, the variations of stopping power and scattering cross sections with energy and a deviation of backscattered spectra from single scattering theory. A summary of the details of this numerical analysis now follows. Let $E_a(z, z')$ be the energy of a backscattered particle, which was dechanneled at z' and backscattered at z, as it leaves the surface of the aligned crystal, and $E_d(z, z')$ be the energy of a particle immediately before scattering at z. The aligned backscattering yield per unit energy interval, denoted as $N_a(E_a)$ may be written as,

$$N_a(E_a) = kIN \sum_{z,z'} [\mathrm{d}\chi(z')\, 1/E_d^2\, \mathrm{d}z/\mathrm{d}E_a] \tag{7}$$

Here $\mathrm{d}\chi(z')$ is the increase in χ in the depth interval $\mathrm{d}z$ at the depth z', k is a proportionality constant, I is the incident beam fluence and N is the atomic density of the crystal. The summation is over all pairs (z', z) which correspond to the same energy E_a and includes all values of z' in the range $0<z'<z_b$, where z_b is the depth at which a particle backscatters immediately after dechanneling and then emerges from the crystal with energy E_a. The product kIN may be written in terms of the random spectrum yield from the near surface region of the crystal, namely,

$$kIN = N_{r,\,0}\, E^2\, [S_{r0}] \tag{8}$$

where $N_{r,\,0}$ is the random yield per unit energy interval due to scattering from the atoms in the near surface region, E is the incident energy and $[S_{r0}]$ is the energy loss factor for scattering of an ion beam from the surface of a randomly oriented crystal. $[S_{r0}]$ is given by

$$[S_{r0}] = K_{M_2}\, S_r(E) + (1/\cos\theta)\, S_r(K_{M_2}E) \tag{9}$$

where S_r is a random stopping power. Combining Eq. (7) with Eq. (8) yields

$$N_a(E_a) = N_{r,\,0}\, E^2[S_{r0}] \sum_{z,z'} [\mathrm{d}\chi(z')\, 1/E_d^2\, \mathrm{d}z/\mathrm{d}E_a] \tag{10}$$

Each term in the sum is formulated by assuming that the particle trajectory contains one scattering collision only (the backscattering) and this is called the single scattering theory. Except for $\mathrm{d}\chi(z')$, all terms in Eq. (10) may be measured or calculated directly. Equation (10) was solved numerically and in sequence starting at the surface, to yield the set of values for $\mathrm{d}\chi$ and hence $\chi(z)$. Corrections (of $\sim$10% magnitude) were also included to take into account the fact that the observed backscattered spectra from a randomly oriented crystal deviate from that calculated according to single

Here $(d\bar{\epsilon}_\perp/dz)$ is the average rate of increase of $\epsilon_\perp$.

In a perfect crystal, there are two principal components of the diffusion function; one due to the interaction of the ion beam with electrons (electronic term) and the other arising from the interaction of the ion beam with thermally vibrating nuclei (nuclear term). As shown by Matsunami and Howe,[6] the average rate of increase of the reduced transverse energy $(d\bar{\epsilon}_\perp/dz)_e$ of the channeled ions due to scattering by electrons can be written as

$$\left(\frac{d\bar{\epsilon}_\perp}{dz}\right)_e = \gamma_e(\epsilon_\perp)\frac{C_e}{Z_e} \tag{15a}$$

with

$$\gamma_e(\epsilon_\perp) = \frac{\langle \rho(\mathbf{r}) L_\psi[\rho(\mathbf{r}), v]\rangle}{(NZ_2 C_e L_e)} \tag{15b}$$

where $\gamma_e(\epsilon_\perp)$ is the electronic reduction function, $\rho(\mathbf{r})$ is the electron density distribution as a function of position $\mathbf{r}$ in the channel, v is the velocity of incident ions, $L_\psi(\rho, v)$ represents the logarithmic term of the mean angular spread[6] and L_e is the usual logarithmic term in stopping power. In Eq. (15a) and Eq. (15b) Z_e and C_e are given by

$$Z_e = \frac{E}{\pi Z_1 e^2 N\, dL_e} \tag{16}$$

and

$$C_e L_e = 1/Z_2 \int \rho(\mathbf{r}) L_\psi\,[\rho(\mathbf{r}), v]\, d\mathbf{r} \tag{17}$$

The diffusion function $D_e(\epsilon_\perp)$ due to scattering of the ion beam by electrons can be written as

$$D_e(\epsilon_\perp) = f_e(\epsilon_\perp)\frac{C_e}{Z_e} \tag{18}$$

where $f_e(\epsilon_\perp)$ is a function derived in Ref. 6. In the present model,[6] it is assumed that there is cylindrical symmetry around the center of the channel as well as the row of atoms (i.e. strings) bordering the channel. The Lindhard approximation to the Thomas–Fermi atomic model was applied in the string region. Because of large uncertainties of the Thomas–Fermi interaction potential, at large distances from the nucleus, a constant electron density ρ_0 was assumed for the electron density in the center region. By separating the electron density distribution into two components (i.e. string and center of channel regions), the geometry of the channel is partly taken into account.

The average increase of the reduced transverse energy of the channeled ions due to interactions with thermally vibrating nuclei is given by

$$\left(\frac{d\bar{\epsilon}_\perp}{dz}\right)_n = \left(\frac{d\bar{\epsilon}_\perp}{dz}\right)_{n,r} \gamma_n(\epsilon_\perp) \tag{19}$$

where $(d\bar{\epsilon}_\perp/dz)_{n,r}$ is the random value, i.e. the value for dechanneled ions, and $\gamma_n(\epsilon_\perp)$ is the nuclear reduction function (see Ref. 6 for analytical expression). The

scattering theory.[7] This was achieved by assuming that the above deviations are due to double scattering of the ion beam within the crystal.[7]

In Figure 2, a comparison is given (for 1.0 MeV ^{1}H ions) between (i) $\chi(z)$ calculated using the detailed numerical analysis (closed symbols and associated curves) and (ii) $\chi(z)$ determined from the ratio of the aligned to random yields (open symbols and associated curves). The two analyses give essentially identical results at shallow depths but diverge to a difference of $\sim 25\%$ at $z=2.5$ μm. Also, the detailed numerical calculation gives a considerably greater dechanneling rate at depths beyond 1.5 μm than does the method of simply taking the ratio of aligned to random yields. Similar behavior was observed for incident ion energies of 0.5, 1.5 and 2.0 MeV. In general, the results indicate that the detailed numerical method is required in the analysis of spectra of backscattered energies less than approximately 0.7 $K_{Au}E$.

3.3 *Theoretical Treatment of Dechanneling*

The theoretical calculations of dechanneling were performed using the diffusion model of Matsunami and Howe[6] and only the salient features of this model are presented here. The particle distribution $g(\epsilon_\perp, z)$ in the reduced transverse energy $\epsilon_\perp$ at a depth z is given by solving the following diffusion equation[4]:

$$\frac{\partial g(\epsilon_\perp, z)}{\partial z} = \frac{\partial}{\partial \epsilon_\perp}\left\{A(\epsilon_\perp)D(\epsilon_\perp)\left[\frac{\partial}{\partial \epsilon_\perp}\frac{g(\epsilon_\perp, z)}{A(\epsilon_\perp)}\right]\right\} \tag{11}$$

Here $A(\epsilon_\perp)$ and $D(\epsilon_\perp)$ are the accessible area where the transverse energy is larger than the continuum potential and the diffusion function, respectively. The reduced transverse energy $\epsilon_\perp = E_\perp/(Z_1 Z_2 e^2/d)$ where $E_\perp$ is the transverse energy. The normalized yield $\chi(z)$ of a close encounter process such as Rutherford scattering is given by

$$\chi(z) = \int_0^\infty g(\epsilon_\perp, z)\, \pi(\epsilon_\perp)\, \mathrm{d}\epsilon_\perp \tag{12}$$

where $\pi(\epsilon_\perp)$ is the probability of a particle with $\epsilon_\perp$ hitting a lattice atom. $\pi(\epsilon_\perp)$ is approximated by the step function

$$\pi(\epsilon_\perp) = \begin{cases} 0 & \epsilon_\perp < \epsilon_\perp{}^c \\ 1 & \epsilon_\perp > \epsilon_\perp{}^c \end{cases} \tag{13}$$

where the critical reduced transverse energy $\epsilon_\perp{}^c = E\psi_{1/2}{}^2/(Z_1 Z_2 e^2/d)$. The diffusion function $D(\epsilon_\perp)$ can be obtained using the following equation:

$$D(\epsilon_\perp) = 1/A(\epsilon_\perp) \int_0^{\epsilon_\perp} A(\epsilon_\perp)\, (\mathrm{d}\bar{\epsilon}_\perp/\mathrm{d}z)\, \mathrm{d}\epsilon_\perp \tag{14a}$$

$$\simeq \int_0^{\epsilon_\perp} (\mathrm{d}\bar{\epsilon}_\perp/\mathrm{d}z)\, \mathrm{d}\epsilon_\perp \tag{14b}$$

ρ_0 was estimated to be 0.6 electrons Å^{-3}. However, there is probably considerable uncertainty in the determination of ρ_0 using Eq. (24) because (1) the harmonic potential is not entirely applicable for the $\langle 110 \rangle$ channel in the f.c.c. lattice where the potential minimum does not occur at the center of the channel, and (2) there are significant differences between ρ_0 values calculated using different atomic potentials. Consequently, in the theoretical dechanneling calculations ρ_0 was treated as a variable fitting parameter. C_n was usually determined using Eq. (22) which yields values of 0.212, 0.254, 0.273 and 0.285 for 0.5, 1.0, 1.5 and 2.0 MeV protons, respectively. The corresponding values of C_n using Eq. (23) are 0.299, 0.288, 0.284 and 0.282. The difference between the theoretical dechanneling curves obtained using C_n values from Eq. (22) and the curves obtained using C_n values from Eq. (23) is $\sim 10\%$ for 0.5 MeV protons and $\lesssim 3\%$ for 1.0, 1.5 and 2.0 MeV protons.

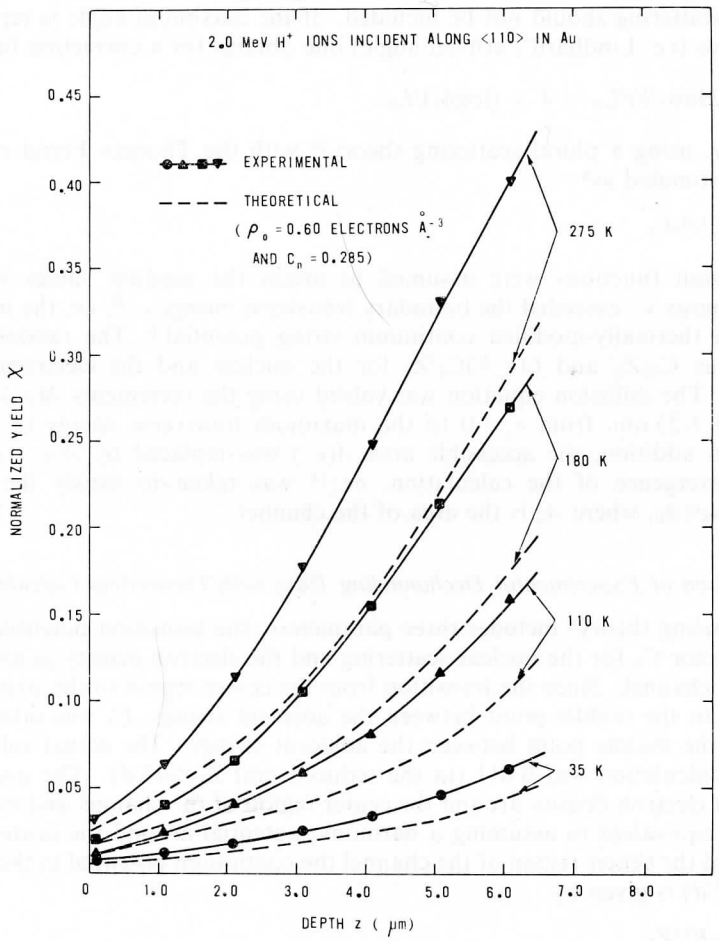

FIGURE 3 Theoretical and experimental results showing the variation of $\chi(z)$ with z for 2.0 MeV protons incident along $\langle 110 \rangle$ in Au at various temperatures. For the theoretical calculations $\rho_0 =$ 0.60 electrons Å^{-3} and $C_n = 0.285$.

random value is written as

$$(\mathrm{d}\bar{\epsilon}_\perp/\mathrm{d}z)_{n,r} = C_n/Z_n \tag{20}$$

with $Z_n = E/2\pi Z_1 Z_2 e^2 N \mathrm{d} L_n$. Here C_n is a correction factor, $L_n = \log(1.29a/b)$, and $b = (Z_1 Z_2 e^2/E)[(M_1+M_2)/M_2]$ is the collision diameter, M_1 and M_2 being the masses of incident ions and target atoms, respectively.

The diffusion function for the nuclear term is given by

$$D_n(\epsilon_\perp) = f_n(\epsilon_\perp)\, C_n/Z_n \tag{21}$$

The analytical expression for $f_n(\epsilon_\perp)$ is also derived in Ref. 6. The dependence on the thermal vibrational amplitude u_2 is contained in the expressions for $\gamma_n(\epsilon_\perp)$ and $f_n(\epsilon_\perp)$.[6] In Eq. (20), $1/Z_n$ is proportional to the integral of the square of the scattering angle multiplied by the scattering cross section which is evaluated from the minimum scattering angle to the maximum scattering angle. For the diffusion process, large angle scattering should not be included. If the maximum angle is replaced by an angle of ψ_1 (i.e. Lindhard's critical angle) one obtains for a correction factor,[6]

$$C_n = \log(1.29a\psi_1/b)/L_n = 1 + (\log\psi_1)/L_n \tag{22}$$

Alternatively, using a plural scattering theory[18] with the Thomas–Fermi cross section, C_n is estimated as[6]

$$C_n \simeq (a\psi_1/b)^{1/3}/L_n \tag{23}$$

The diffusion functions were assumed to attain the random values when the transverse energy $\epsilon_\perp$ exceeded the boundary transverse energy $\epsilon_\perp{}^B$, i.e. the maximum value of the thermally-modified continuum string potential.[6] The random values were taken as C_n/Z_n and $f_e(\epsilon_\perp{}^B)C_e/Z_e$ for the nuclear and the electronic terms, respectively. The diffusion equation was solved using the increments $\Delta(\epsilon_\perp)^{1/2}=0.02$ and $\Delta z = 0.5$–1.25 nm, from $\epsilon_\perp = 0$ to the maximum transverse energy ($\epsilon_\perp{}^m \sim 2\epsilon_\perp{}^B$ to $3\epsilon_\perp{}^B$). In addition, the accessible area $A(\epsilon_\perp)$ was replaced by $A(\epsilon_\perp + \delta\epsilon_\perp{}^{th})$ to avoid the divergence of the calculation. $\delta\epsilon_\perp{}^{th}$ was taken to satisfy the relation $A(\delta\epsilon_\perp{}^{th}) = \pi u_2{}^2/A_0$, where A_0 is the area of the channel.

3.4 *Comparison of Experimental Dechanneling Data with Theoretical Calculations*

The dechanneling theory[6] includes three parameters: the transition potential U_t, the correction factor C_n for the nuclear scattering and the electron density ρ_0 around the center of the channel. Since the transition from the center region to the string region occurs close to the middle point between the adjacent strings, U_t was taken as the potential at the middle point between the adjacent strings. The actual value of U_t used in the calculation was 0.011 (in the reduced unit $Z_1 Z_2 e^2/d$). The assumption of a constant electron density around the center region of the channel and cylindrical symmetry is equivalent to assuming a harmonic potential around the center region. Hence around the center region of the channel the continuum potential in the reduced unit $(Z_1 Z_2 e^2/d)$ is given by

$$U(R) = \pi \mathrm{d} \rho_0 R^2/Z_2 \tag{24}$$

where the distance R is measured from the center of the channel. From Eq. (24) an estimate can be made of the electron density ρ_0. Based upon the Molière potential

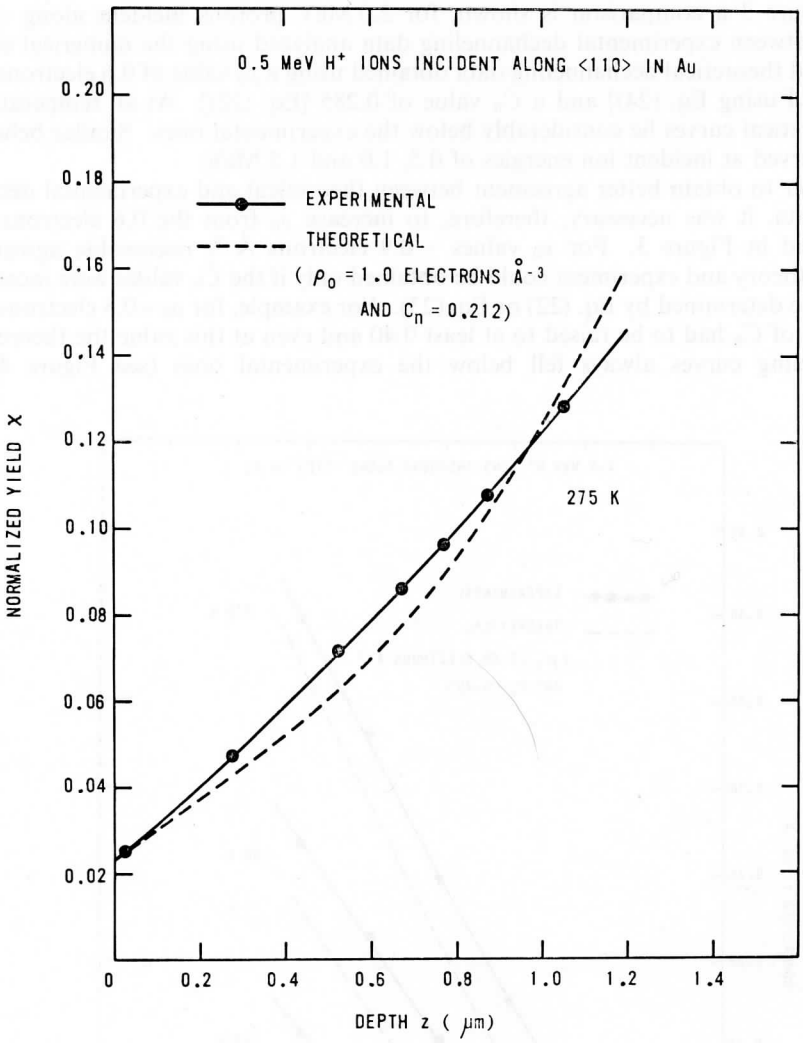

FIGURE 5 Theoretical and experimental results showing the variation of $\chi(z)$ with z for 0.5 MeV protons incident along $\langle 110 \rangle$ in Au at 275 K. For the theoretical calculations $\rho_0 = 1.0$ electrons Å^{-3} and $C_n = 0.212$.

example). $C_n = 0.40$ also represents an effective upper limit for this parameter as larger C_n values give rise to unrealistic results in the theoretical calculations. At $\rho_0 = 1.0$ electrons Å^{-3} good agreement between theory and experiment was obtained using C_n values calculated from Eq. (22) [or Eq. (23)]. This was true for the whole range of incident ion energies (0.5–2.0 MeV) and crystal temperatures (35 to 275 K) which were investigated, as illustrated in Figures 5–8.

In Figures 3–8 the theoretical dechanneling curves were compared with experimental curves derived using the numerical analysis outlined in Section 3.2. If the comparison is made between the theoretical $\chi(z)$ values and experimental $\chi(z)$ values

In Figure 3 a comparison is shown, for 2.0 MeV protons incident along ⟨110⟩ in Au, between experimental dechanneling data analyzed using the numerical calculation and theoretical dechanneling data obtained using a ρ_0 value of 0.6 electrons Å^{-3} [estimated using Eq. (24)] and a C_n value of 0.285 [Eq. (22)]. At all temperatures, the theoretical curves lie considerably below the experimental ones. Similar behavior was observed at incident ion energies of 0.5, 1.0 and 1.5 MeV.

In order to obtain better agreement between theoretical and experimental dechanneling data, it was necessary, therefore, to increase ρ_0 from the 0.6 electrons Å^{-3} value used in Figure 3. For ρ_0 values $\lesssim$0.9 electrons Å^{-3}, reasonable agreement between theory and experiment could be obtained only if the C_n values were increased over those determined by Eq. (22) or Eq. (23). For example, for ρ_0=0.8 electrons Å^{-3} the value of C_n had to be raised to at least 0.40 and even at this value the theoretical dechanneling curves always fell below the experimental ones (see Figure 4 for

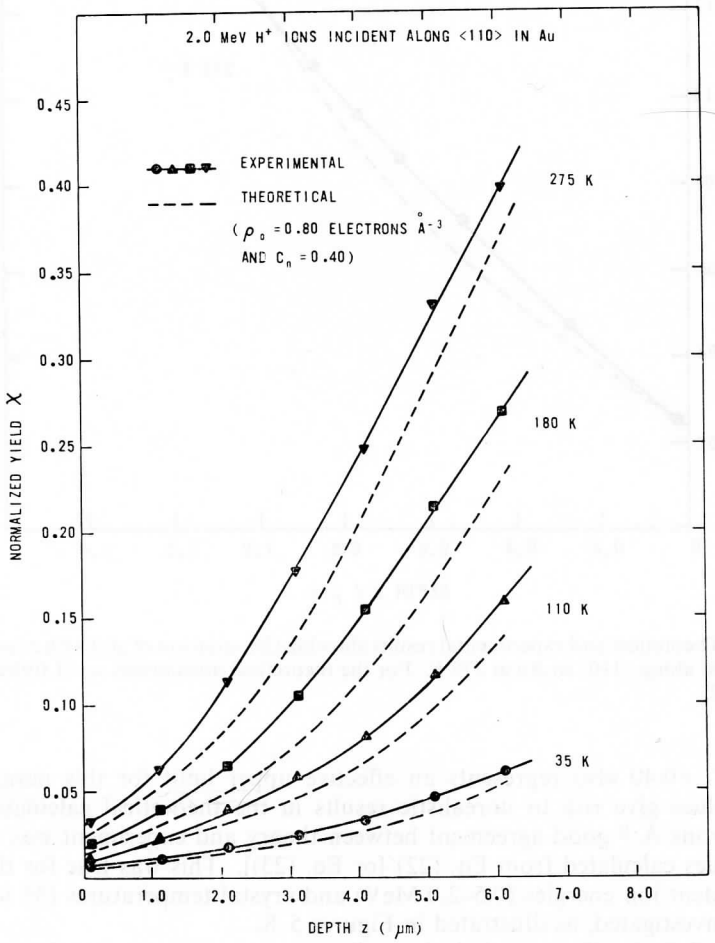

FIGURE 4 Theoretical and experimental results showing the variation of $\chi(z)$ with z for 2.0 MeV protons incident along ⟨110⟩ in Au at various temperatures. For the theoretical calculations ρ_0= 0.80 electrons Å^{-3} and C_n=0.40.

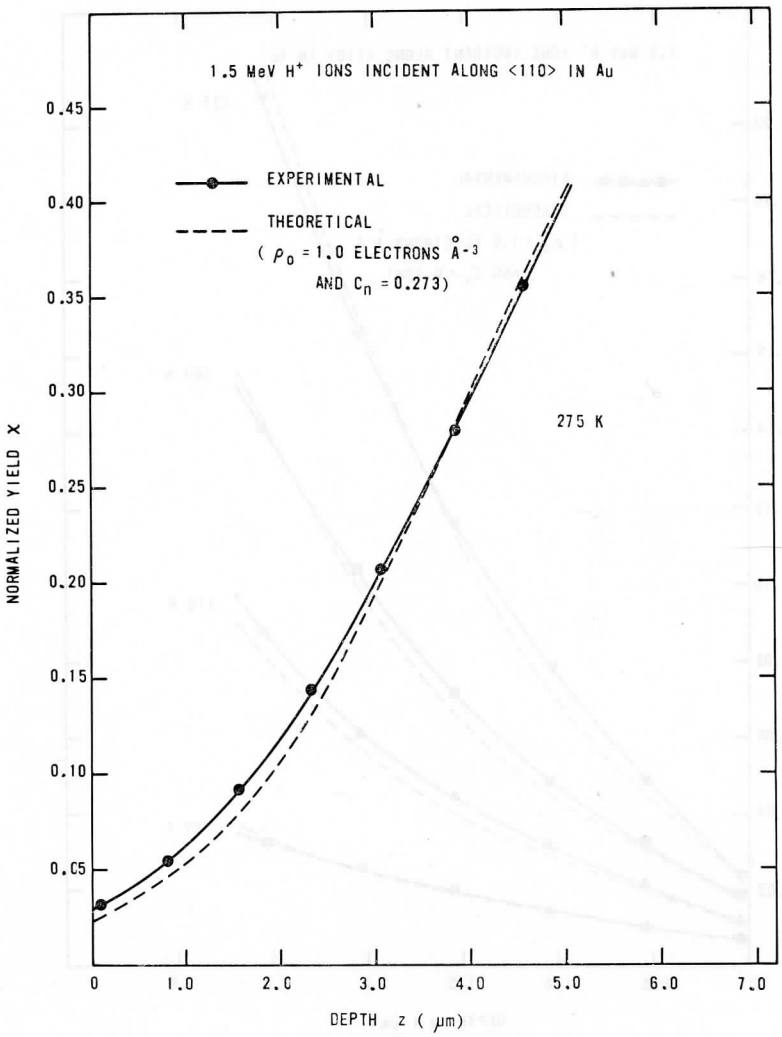

FIGURE 7 Theoretical and experimental results showing the variation of $\chi(z)$ with z for 1.5 MeV protons incident along $\langle 110 \rangle$ in Au at 275 K. For the theoretical calculations $\rho_0 = 1.0$ electrons Å^{-3} and $C_n = 0.273$.

diverge appreciably at greater depths. In general, for all incident ion energies and crystal temperatures investigated, the numerical analysis treatment of the dechanneling data gave the better overall fit to the theoretical dechanneling calculations.

A striking feature of dechanneling in Au is the observed strong dependence of $\chi(z)$ and $d\chi(z)/dz$ on the temperature. Consider, for example, the experimental dechanneling curves for 1.0 MeV protons plotted in Figure 6. At a penetration depth of 2 μm, an increase in the crystal temperature from 35 K to 275 K resulted in increases in $\chi(z)$ and $d\chi(z)/dz$ by factors of approximately 6 and 10, respectively. Inspection of Figures 6 and 8 show that the variation of $\chi(z)$ with temperature, at

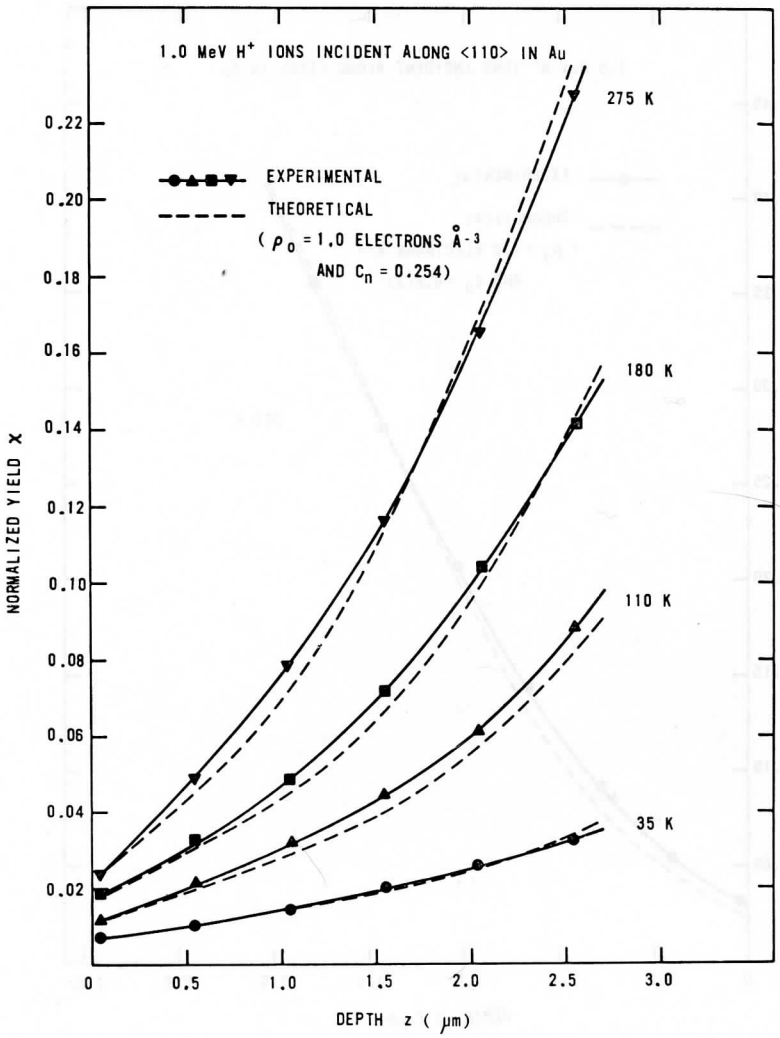

FIGURE 6 Theoretical and experimental results showing the variation of $\chi(z)$ with z for 1.0 MeV protons incident along $\langle 110 \rangle$ in Au at various temperatures. For the theoretical calculations $\rho_0 =$ 1.0 electrons Å^{-3} and $C_n = 0.254$

obtained directly from the ratio of the aligned to random yields, then even for favorable combinations of the ρ_0 and C_n parameters [e.g. $\rho_0 = 0.8$ and $C_n = 0.4$ or $\rho_0 = 1.0$ and C_n determined from Eq. (22)] good agreement between theory and experiment is observed only over penetration depths where the energy of the backscattered protons was greater than $\sim 0.6\, K_{Au}E$. At larger depths of penetration, the theoretical curves have a considerably greater slope (i.e. dechanneling rate) than the experimental curves. An example of this behavior is shown in Figure 9 for 1.0 MeV protons where it can be seen that the theoretical and experimental curves nearly coincide at depths up to $\sim 1.75\, \mu$m (backscattered proton energy $\sim 0.6\, K_{Au}E$) but start to

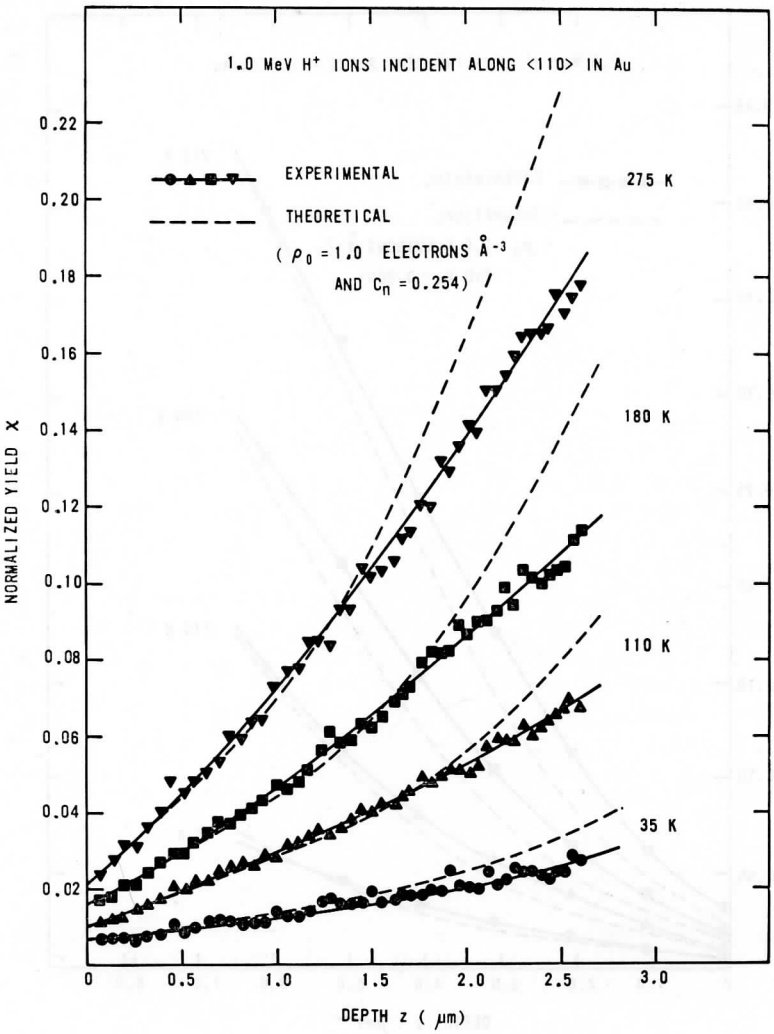

FIGURE 9 Theoretical and experimental results showing the variation of $\chi(z)$ with z for 1.0 MeV protons incident along $\langle 110 \rangle$ in Au at various temperatures. The experimental $\chi(z)$ values were determined from the ratio of the aligned yield to the random yield. For the theoretical calculations $\rho_0 = 1.0$ electrons Å^{-3} and $C_n = 0.254$.

continuum potential. If the 11 outer electrons ($5d^{10}\,6s$) of the Au atoms were uniformly distributed throughout the lattice, this would give rise to an electron density of 0.65 electrons Å^{-3}. Previously, Matsunami and Howe[6] used $\rho_0 = 0.10$ Å^{-3} and $\rho_0 = 0.13$ Å^{-3} as the values to give good agreement between theoretical and experimental dechanneling curves in Si for the $\langle 110 \rangle$ and $\langle 111 \rangle$ channels, respectively. These values were in quite good agreement with the electron densities estimated from the harmonic approximation which gave $\rho_0 = 0.08$ and $\rho_0 = 0.15$ electrons Å^{-3} for the $\langle 110 \rangle$ and $\langle 111 \rangle$ channels, respectively. In Ge, they[6] found that

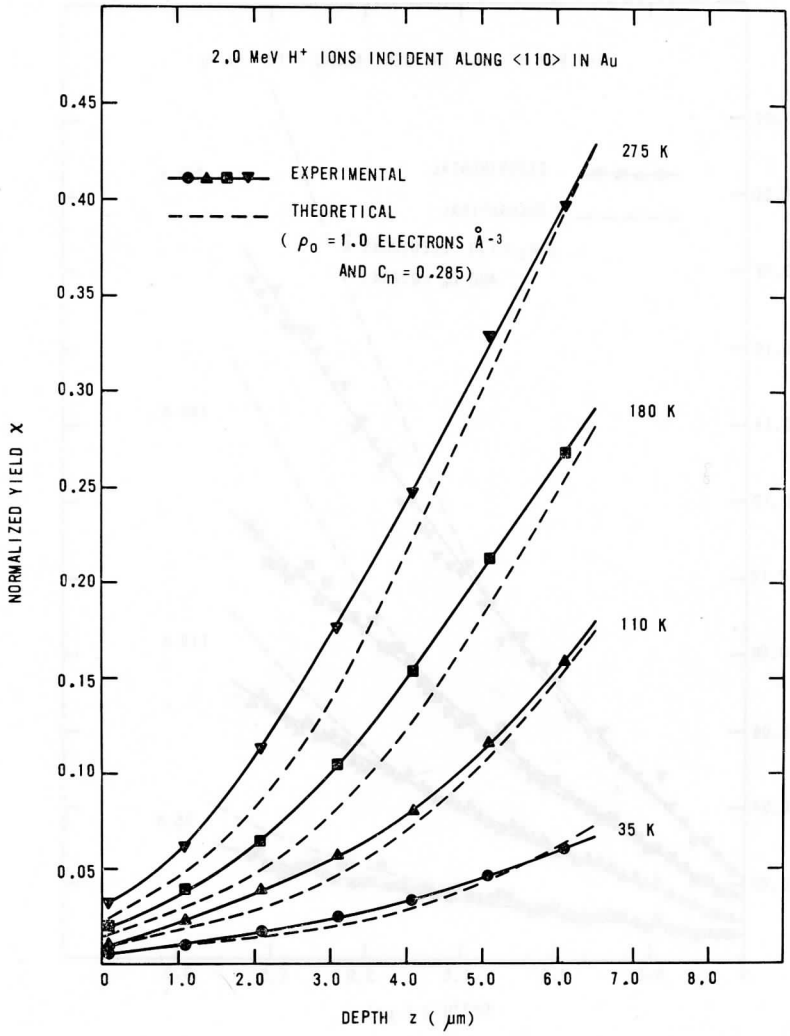

FIGURE 8 Theoretical and experimental results showing the variation of $\chi(z)$ with z for 2.0 MeV protons incident along $\langle 110 \rangle$ in Au at various temperatures. For the theoretical calculations $\rho_0 = 1.0$ electrons Å^{-3} and $C_n = 0.285$.

constant depth, is very well described by the theory. This supports the theoretical description of nuclear scattering used in the diffusion channeling theory by Matsunami and Howe.[6]

In the present treatment ρ_0 was treated as a variable fitting parameter since electron densities in the central regions of the channels have not been determined experimentally. The values of 0.8–1.0 electrons Å^{-3} which are required to yield reasonable agreement between theoretical and experimental dechanneling data in $\langle 110 \rangle$ Au (depending upon the choice of C_n values) were 33–66% larger than the value of 0.6 electrons Å^{-3} estimated by assuming a harmonic approximation to the Molière

the value of ρ_0 giving the best agreement between theory and experiment was 0.12 Å^{-3} for both the ⟨110⟩ and ⟨111⟩ channels which is to be compared with values of 0.08 Å^{-3} and 0.22 Å^{-3} for the ⟨110⟩ and ⟨111⟩ axes, respectively, as estimated using Eq. (24). If the outer electrons in Si ($3s^2\,3p^2$) and Ge ($4s^2\,4p^2$) were uniformly distributed throughout the lattice the resulting electron densities would be 0.20 and 0.18 electrons Å^{-3}, respectively. To what extent the "best fit" value of ρ_0 deduced from the dechanneling calculations would be affected by using a non-harmonic potential in place of Eq. (24) in the Matsunami and Howe[6] treatment has yet to be determined. Certainly the harmonic potential is more applicable to the ⟨110⟩ and ⟨111⟩ channels of the diamond structure (Si, Ge) than to the ⟨110⟩ channel of the f.c.c. structure (Au).

3.5 *Conclusions*

For the ⟨110⟩ axis in Au, dechanneling data have been obtained in very good quality gold crystals, at various temperatures and for different energies of the incident proton beam. The experimental data were analyzed using the normal method of determining the normalized backscattered yield $\chi(z)$ from the ratio of the aligned to random spectra as well as a numerical method which also takes into account the deviation of the backscattered spectra from single scattering theory. Theoretical dechanneling curves were obtained by computation using the diffusion model of Matsunami and Howe.[6] This included modifying the electron density ρ_0 around the center of the channel and applying a correction factor C_n for the nuclear scattering. Best overall agreement was obtained between theory and the experimental data analyzed using the numerical method. The observed strong temperature dependence of $\chi(z)$ and the dechanneling rate $d\chi(z)/dz$ are well described by the theory within the uncertainties of measurement and theory (10%). Values of ρ_0 required to give good agreement between theory and experiment were in the region 0.8–1.0 electrons Å^{-3}.

ACKNOWLEDGEMENTS

The authors wish to thank J. A. Davies and I. V. Mitchell for comments on the manuscript. The technical assistance of A. F. Quenneville in preparing the single crystal specimens used in the investigation was also greatly appreciated.

REFERENCES

1. J. Lindhard, *Mat. Fys. Medd.* **34,** No.14 (1965).
2. F. Grasso, *Channeling*, D. V. Morgan (Ed.) (John Wiley & Sons Ltd., 1973), p. 181.
3. D. S. Gemmell, *Rev. Mod. Phys.* **46,** 129 (1974).
4. H. E. Schiøtt, E. Bonderup, J. U. Andersen, and H. Esbensen, *Atomic Collisions in Solids*, 1973 Gatlinburg Conf., S. Datz *et al.* (Eds.) (Plenum Press, 1975), Vol. 2, p. 843.
5. M. J. Pedersen, J. U. Andersen, D. J. Elliott, and E. Laesgaard, *Atomic Collisions in Solids*, 1973 Gatlinburg Conf., S. Datz *et al.* (Eds.) (Plenum Press, 1975), Vol. 2, p. 863.
6. N. Matsunami and L. M. Howe, *Rad. Eff.* **51,** 111 (1980).
7. J. A. Moore, *Nucl. Instr. Meth.* **174,** 577 (1980).
8. J. Bøttiger, J. A. Davies, J. Lori, and J. L, Whitton, *Nucl. Instr. Meth.* **109,** 579 (1973).
9. M. L. Swanson, P. Offermann, and K. H. Ecker, *Can. J. Phys.* **57,** 457 (1979).
10. K. L. Merkle, P. P. Pronko, D. S. Gemmell, R. C. Mikkelson, and J. R. Wrobel, *Phys. Rev.* **B8,** 1002 (1973).
11. J. H. Barrett, *Phys. Rev.* **B3,** 1527 (1971).
12. *International Tables for X-ray Crystallography* (Kynock Press, 1962), Vol. III, p. 234.

13. J. L'Ecuyer, J. A. Davies, and N. Matsunami, *Nucl. Instr. Meth.* **160,** 337 (1979).
14. L. C. Feldman, *Nucl. Instr. Meth.* **191,** 211 (1981).
15. E. Bøgh, *Can. J. Phys.* **46,** 653 (1968).
16. J. Bøttiger and F. H. Eisen, Ion beam surface layer analysis, *Proc. 1978 Yorktown Heights Conf.* (Elsevier Sequoia, S.A., 1974), p. 239.
17. H. H. Andersen and J. F. Ziegler, *Hydrogen Stopping Power and Ranges in All Elements*, (Pergamon Press, 1977).
18. L. Meyer, *Phys. Stat. Sol.* **B44,** 253 (1971).